

Can nonstandard neutrino interactions explain the XENON1T spectral excess?

Amir N. Khan^{1,*}

¹Max-Planck-Institut für Kernphysik, Postfach 103980, D-69029 Heidelberg, Germany

(Dated: July 6, 2022)

We perform a spectral analysis of the excess observed in the recoiled electron energy spectrum by XENON1T with nonstandard neutrino interactions. To this aim we consider the neutrino magnetic moment, charge radius and new light vector and scalar mediators and compare their effects on the spectrum. We find that the excess can be explained in the range $(2-4) \times 10^{-11} \mu_B$ for the magnetic moment, $(2-6) \times 10^{-31} \text{cm}^2$ for the charge radius, and $(10-100) \text{keV}$ masses of light mediators, couplings of about 5×10^{-7} and 1.2×10^{-6} for vector and scalar mediators, respectively, however, some of these limits are in tension with the bounds from other laboratory experiments.

I. INTRODUCTION

Recently, the XENON1T has observed an excess in the recoiled electron energy spectrum [1]. Above the known and expected Standard Model background, more events than expected were observed in the $(1-7) \text{keV}$ region of electron recoil. The large exposure and unprecedentedly low background rate of the experiment could indeed enable fundamental discoveries. Or enable the discovery of a new background source.

Several phenomenological papers appeared immediately after the announcement of the collaboration [1]. This is one of them. We investigate the possibility that neutrinos possess new interactions that modify the neutrino-electron cross section at the low energies probable by XENON1T. Already in the XENON1T paper [1], the possibility of an enhanced neutrino magnetic, although in comparison to *only* Borexino limit, was analyzed, besides solar axions, bosonic dark matter and a possible new background source, tritium.

With spectral analysis we explain this interesting excess with the help of nonstandard standard neutrino interactions (NSI) by considering bounds from reactor, accelerator, solar and COHERENT experiments [2-8]. The possibilities we discuss are a neutrino magnetic moment, a neutrino charge radius, and the presence of light scalar and vector mediators that mediate neutrino-electron scattering. We will show that how does these four new physics choices compete with each other to explain the spectral shape of the recoil excess. We will also discuss how does the constraints on neutrino magnetic moment and neutrino charge radius are in tension with the bounds from other laboratory experiments, particularly from COHERENT experiment[4, 5].

II. EXPECTED NSI SPECTRUM

Here we recap the important formulas needed for our calculations of the nonstandard neutrino interaction ef-

fects. We split them into neutrino electromagnetic properties and light mediators in the neutrino-electron interactions.

(1) $\nu_\alpha - e$ weak and electromagnetic scattering cross-sections- The total differential cross section for the $\nu - e$ scattering is

$$\frac{d\sigma_{\nu_\alpha e}}{dE_r} = \left(\frac{d\sigma_{\nu_\alpha e}}{dE_r} \right)_{SM} + \left(\frac{d\sigma_{\nu_\alpha e}}{dE_r} \right)_{MM}, \quad (1)$$

where

$$\left(\frac{d\sigma_{\nu_\alpha e}}{dE_r} \right)_{SM} = \frac{2G_F^2 m_e}{\pi} [g_L^2 + g_R^2 \left(1 - \frac{E_r}{E_\nu} \right)^2 - g_L g_R \frac{m_e E_r}{E_\nu^2}] \quad (2)$$

is the standard electroweak cross section and

$$\left(\frac{d\sigma_{\nu_\alpha e}}{dE_r} \right)_{MM} = \frac{\pi \alpha_{em}^2 (\mu_\nu^{eff})^2}{m_e^2} \left[\frac{1}{E_r} - \frac{1}{E_\nu} \right] \quad (3)$$

is the neutrino magnetic moment cross section [9-12]. Here, G_F is Fermi constant, $g_{L(R)} = (g_V \mp g_A)/2 + 1$ for ν_e and $g_{L(R)} = (g_V \mp g_A)/2$ for ν_μ and ν_τ , $g_V = -1/2 + \sin^2 \theta_W$, $g_A = -1/2$, μ_ν is the effective neutrino magnetic moment in units of Bohr magneton (μ_B), α_{em} is the fine-structure constant, m_e is the electron mass, E_ν is the incoming neutrino energy and E_r is the recoiled electron energy in the detector. We take $\sin^2 \theta_W = 0.23126$ in the $\overline{\text{MS}}$ scheme [13] with the tiny radiative corrections less than 2% included. For neutrino charge radius we simply replace g_V by $g_V \rightarrow g_V + (\sqrt{2} \alpha_{em} / 3G_F) \langle r_{\nu_\alpha}^2 \rangle$ [9-12].

(2) Light vector and scalar mediators- For simplicity we assume that new light mediators couple with equal strength to both neutrinos and electron. Also, we neglect the pseudo-scalar and axial-vector contribution. For the vector type mediator, in the low momentum transfer limit, we replace g_V as [6, 7]

$$g_V \rightarrow g_V + \left(\frac{g_{Z'}^2}{2\sqrt{2}G_F(2m_e E_r + m_{Z'})} \right), \quad (4)$$

in the standard model cross section of the eqn. 2, where $g_{Z'}$ is the coupling constant and $m_{Z'}$ is the mass of the

* amir.khan@mpi-hd.mpg.de

vector mediator. For scalar mediators we add their contribution to the standard model cross section incoherently. The scalar interaction cross therefore is

$$\left(\frac{d\sigma_{\nu_\alpha e}}{dE_r} \right)_{scalar} = \left(\frac{g_\phi^4}{4\pi(2m_e E_r + m_\phi)^2} \right) \frac{m_e^2 E_r}{E_\nu^2}, \quad (5)$$

$$\frac{dN}{dE_{rec}} = n_e \times \int_{E_\nu^{mn}}^{E_\nu^{mx}} dE_\nu \int_{E_r^{th}}^{E_r^{mx}} dE_r \left(\frac{d\sigma_{\nu_e e}}{dE_r} P_{ee}^m + \frac{d\sigma_{\nu_\mu/\tau e}}{dE_r} P_{e\mu/\tau}^m \right) \times \frac{d\phi}{dE_\nu} \times \epsilon(E_r) \times G(E_r, E_{rec}), \quad (6)$$

where $G(E_r, E_{rec})$ is a normalized Gaussian smearing function to account for the detector finite energy resolution with resolution power $\sigma(E_r)/E_r = (0.3171/\sqrt{E_r[\text{keV}]}) + 0.0015$ and $\epsilon(E_r)$ is the detector efficiency both taken from [1, 14], $d\phi/dE_\nu$ is the solar flux spectrum taken from [15] and n_e is the number of target electrons in fiducial volume of one ton Xenon [1]. Here, $d\sigma_{\nu_\alpha e}/dE_r$ are cross sections given in eqn. 2 above, P_{ee}^m and $P_{e\mu/\tau}^m$ are the survival and conversion probabilities of solar pp electron neutrino including the negligibly small matter effects given as

$$P_{ee}^m = s_{13}^4 + \frac{1}{2} c_{13}^4 (1 + \cos 2\theta_{12}^m \cos 2\theta_{12}) \quad (7)$$

and $P_{e\mu/\tau}^m = 1 - P_{ee}^m$, where s_{ij} , c_{ij} are mixing angles in vacuum and θ_{12}^m is the matter effects induced mixing angle taken from [16, 17]. We consider the maximal mixing case for the conversion probability. The integration limits are $E_\nu^{mn} = (E_r + \sqrt{2m_e E_r + E_r^2})/2$ and $E_\nu^{mx} = 420$ keV, the pp neutrinos spectrum limit, $E_r^{th} = 1$ keV is the detector threshold and $E_r^{mx} = 30$ keV is the maximum recoil energy for the region of interest.

III. RESULTS AND DISCUSSION

Equipped with all the necessary formulas given above we calculate the differential event rate energy spectrum as function of E_{rec} for the standard model case and then for our new physics cases, that is, neutrino magnetic moment, neutrino charge radius, light vector and scalar mediators. First, we made sure to reproduce the expected spectrum of fig.1 of ref. [1] corresponding to $\mu_\nu = 7 \times 10^{-11} \mu_B$ including the true energy smearing and the efficiency of the detector using our eqn. 6. Our SM expected energy spectrum shown in black color in both fig. 1 and 2 also agree very well with the expected spectrum given in ref. [18].

We then add the neutrino magnetic moment, neutrino charge radius, light vector and scalar mediators each one at a time and choose bench mark values of new physics parameters in each case within ranges of the current bounds [5–7, 19, 20]. For each case we choose three values

where g_ϕ is the coupling constant and m_ϕ is mass of the scalar mediators.

Next we define the differential event rate in terms of the reconstructed recoiled energy (E_{rec}) in order to estimate the contribution of the aforementioned new physics to the recoiled electron spectrum. This can be written as **(Note Added)**

which lie in 1σ of the experimental data of XENON1T as shown fig. 1 and fig. 2. Our new physics expected results are shown in the continuous blue, orange and green color in both figures.

In Fig.1(left), we show the neutrino magnetic moment case and choose three values $(2, 3, 4) \times 10^{-11} \mu_B$. In Fig.1(right), we show our expected spectrum for neutrino charge radius for the bench mark values $(2, 4, 6) \times 10^{-31} \text{cm}^2$. One can see that excess is better explained by neutrino magnetic moment while the charge radius contribution has a flat increase with in the spectrum. This is because the neutrino magnetic moment cross section is sensitive at low recoils while the charge radius section cross section is not competitively sensitive at low recoils as can be see from the cross section formulas in eqn. 1 and 2. However, charge radius do have a substantial contribution in the excess region and cannot be ignored.

In Fig.2, we show light mediator contributions for three bench mark mass values of $(10, 50, 100)$ keV with coupling constants of 5×10^{-7} for vector (left) and 1.2×10^{-7} for scalars (right). One can see that for the chosen set of mass values, which are same for both cases, the scalar mediators have spectral increase in $(1 - 15)$ keV region, while the vector mediators spectrum increase in the range $(1 - 10)$ keV. Again, vector mediators have smooth fitting to the spectrum specially in the excess region of $(1 - 7)$ keV.

IV. CONCLUSIONS

We did a spectral analysis to explain the excess observed in the electron recoil energy spectrum in XENON1T detector with neutrino nonstandard interactions. We have considered four different new physics cases 1) neutrino magnetic moment 2) charge radius 3) light vector 4) scalar mediators. We use the current ranges of the new physics parameters bounds to interpret the observed excess. Our analysis shows that the boundaries of neutrino magnetic moment and charge radius considered here are in *tension* with the recent constraints (see Table II and IV of ref. [4]) from the COHERENT data in particular. The bounds on neutrino

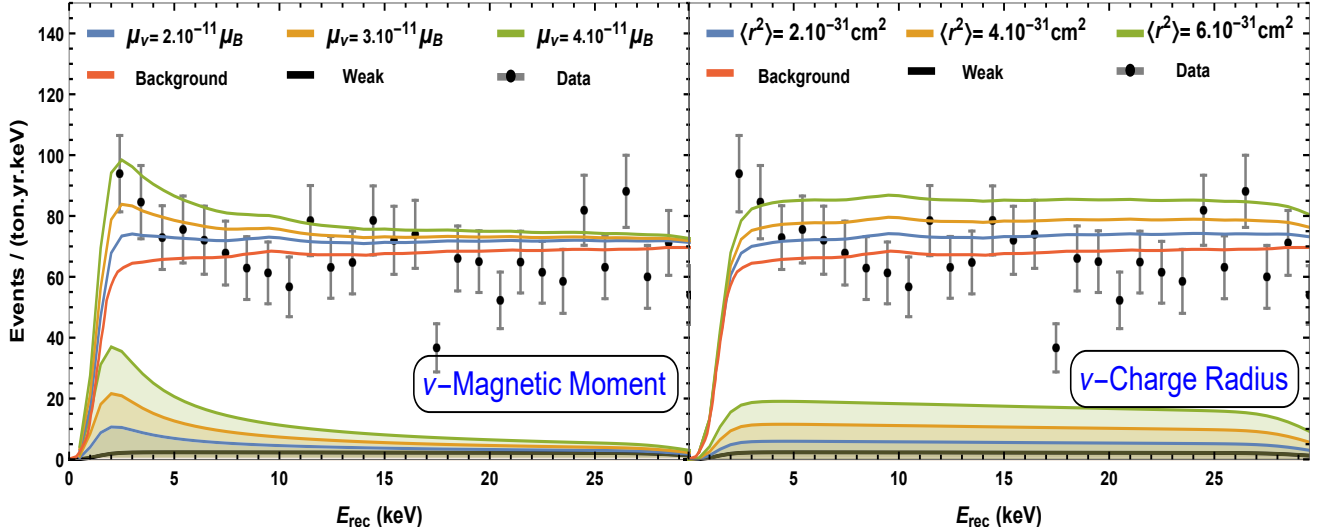


FIG. 1. Experimental data, backgrounds, SM energy spectrum and our expected spectrum for different values neutrino magnetic moment (left) and neutrino charge radius (right). Different graphs can be read from the legends inside each figure. The shaded regions in the bottom correspond to the expectation without any backgrounds while the continuous line graphs correspond to the expectation+background. The data points and background were taken from ref. [1].

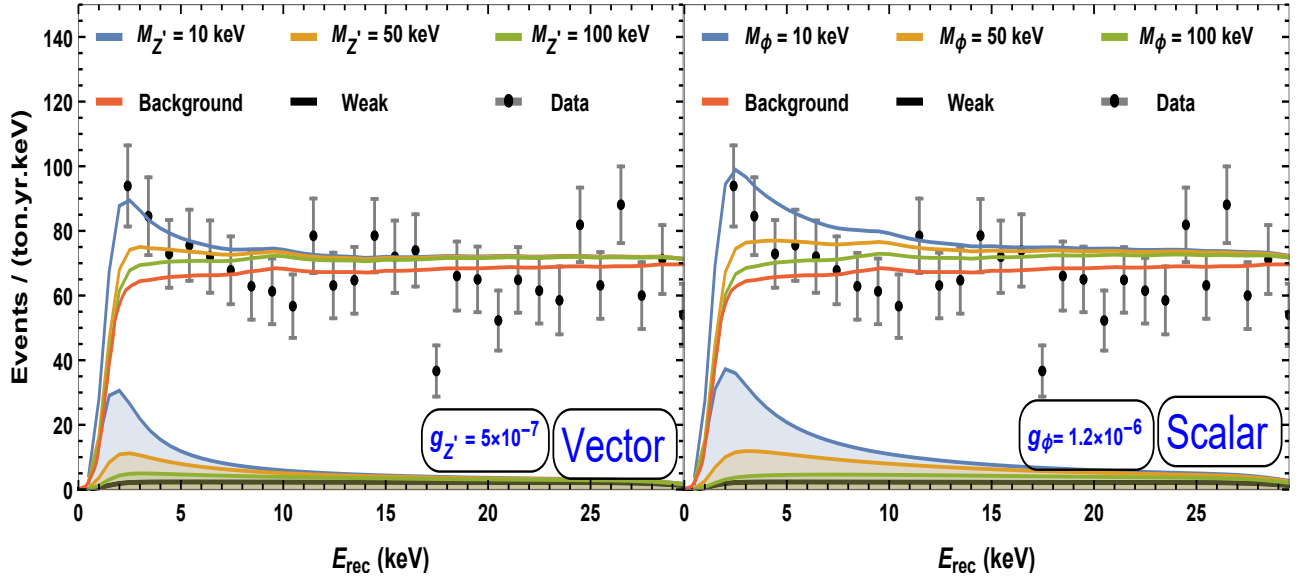


FIG. 2. Experimental data, backgrounds, SM energy spectrum and our expected spectrum for different values of the light vector mediators (left) and scalar mediators (right). Different graphs can be read from the legends in inside each figure. The shaded regions in the bottom correspond to the expectation without any backgrounds while the continuous line graphs correspond to the expectation+background. The data points and background were taken from ref. [1].

magnetic moment obtained in ref. [4] are too large to explain the excess here, while those on charge radius are too tight to explain this excess. This implies that more stringent constraints expected on neutrino magnetic moment but relatively weaker on charge radius are expected from the XENON1T data. We leave the fitting analysis for a follow up work.

For the light mediators, due to a large allowed free parameter space of masses and couplings constants the excess be explained with arbitrary but reasonable choices already determined by other experiments. In this case we find that the whole spectrum, but the excess region in particular, is sensitive to variation in a very narrower window of the parameter boundaries considered here.

We find that within 1σ experimental uncertainty the excess region of $(1 - 7)$ keV is better explained in the range $(2 - 4) \times 10^{-11} \mu_B$ for magnetic moment, $(2 - 6) \times 10^{-31} \text{cm}^2$ for charge radius, $(10 - 100)$ keV mass ranges with couplings of 5×10^{-7} and 1.2×10^{-6} for vector and scalar mediators, respectively. Out of the considered four different physics scenarios, neutrino magnetic moment and the light vector type mediators fit better to the observed excess.

We conclude that neutrino nonstandard interactions could be the top candidate to explain the excess given the fact that neutrinos are massive and could have new

interactions beyond the standard model unless this possibility is excluded by other experiments .

V. NOTE ADDED

While preparing this manuscript, paper [21] appeared on arXiv which overlap partially to this work. We have noticed that they either ignored the detector energy resolution, detection efficiency and the oscillation probabilities or they have not treated them properly. About the oscillation probability, the correct estimation is possible with the form given in eqn. (6) here. However, they only consider the survival part and ignore the conversion rates in the detector. Also they do not take any energy dependence of the oscillation probabilities, which although small for pp neutrinos, but cannot be ignored entirely to get correct results.

ACKNOWLEDGMENTS

The author thanks Werner Rodejohann for useful discussions. This work is financially supported by Alexander von Humboldt Foundation under the postdoctoral fellowship program.

[1] E. Aprile *et al.* (XENON), (2020), arXiv:2006.09721 [hep-ex].

[2] M. Deniz *et al.* (TEXONO), Phys. Rev. D **81**, 072001 (2010), arXiv:0911.1597 [hep-ex].

[3] C. Giunti, K. A. Kouzakov, Y.-F. Li, A. V. Lokhov, A. I. Studenikin, and S. Zhou, Annalen Phys. **528**, 198 (2016), arXiv:1506.05387 [hep-ph].

[4] M. Cadeddu, F. Dordei, C. Giunti, Y. Li, E. Picciano, and Y. Zhang, (2020), arXiv:2005.01645 [hep-ph].

[5] A. N. Khan and W. Rodejohann, Phys. Rev. D **100**, 113003 (2019), arXiv:1907.12444 [hep-ph].

[6] M. Lindner, F. S. Queiroz, W. Rodejohann, and X.-J. Xu, JHEP **05**, 098 (2018), arXiv:1803.00060 [hep-ph].

[7] G. Arcadi, J. Heeck, F. Heizmann, S. Mertens, F. S. Queiroz, W. Rodejohann, M. Slezak, and K. Valerius, JHEP **01**, 206 (2019), arXiv:1811.03530 [hep-ph].

[8] *Neutrino Non-Standard Interactions: A Status Report*, Vol. 2 (2019) arXiv:1907.00991 [hep-ph].

[9] K. Fujikawa and R. Shrock, Phys. Rev. Lett. **45**, 963 (1980).

[10] P. Vogel and J. Engel, Phys. Rev. D **39**, 3378 (1989).

[11] M. Dvornikov and A. Studenikin, Phys. Rev. D **69**, 073001 (2004), arXiv:hep-ph/0305206.

[12] M. S. Dvornikov and A. I. Studenikin, J. Exp. Theor. Phys. **99**, 254 (2004), arXiv:hep-ph/0411085.

[13] J. Erler and M. J. Ramsey-Musolf, Phys. Rev. D **72**, 073003 (2005), arXiv:hep-ph/0409169.

[14] E. Aprile *et al.* (XENON), (2020), arXiv:2003.03825 [physics.ins-det].

[15] J. N. Bahcall and C. Pena-Garay, New J. Phys. **6**, 63 (2004), arXiv:hep-ph/0404061.

[16] I. Lopes and S. Turck-Chizé, Astrophys. J. **765**, 14 (2013), arXiv:1302.2791 [astro-ph.SR].

[17] P. Z. *et al.* (Particle Data Group), to be published in Prog. Theor. Exp. Phys. 2020, 083C01 (2020).

[18] E. Shockley, <https://www.dropbox.com/s/vrq49tldjdfvnjh/shockley20200617.pdf?dl=0> (June 17th, 2020).

[19] M. Agostini *et al.* (Borexino), Phys. Rev. D **96**, 091103 (2017), arXiv:1707.09355 [hep-ex].

[20] A. N. Khan, J. Phys. G **46**, 035005 (2019), arXiv:1709.02930 [hep-ph].

[21] C. Boehm, D. G. Cerdeno, M. Fairbairn, P. A. Machado, and A. C. Vincent, (2020), arXiv:2006.11250 [hep-ph].